

BRIEF REPORT

Open Access



# A primary insight into gut microbiome, MicroRNA and stemness, in a PCOS rat model

Fereshteh Esfandiarienezhad<sup>1,2,3†</sup>, Xiaoshu Zhan<sup>4,5†</sup>, Seang Lin Tan<sup>3,6</sup>, Julang Li<sup>4\*</sup> and Benjamin K. Tsang<sup>1,2\*</sup>

## Abstract

Polycystic ovary syndrome (PCOS) is a common endocrine disorder associated with reproductive and metabolic dysfunctions, including gut microbiome dysbiosis. This study aimed to examine the alterations in stemness in ovarian surface epithelium (OSE), gut microbiome microRNA expression in granulosa cells and plasma in a dihydrotestosterone (DHT)-induced rat model of PCOS. Female rats were administered DHT to induce PCOS, and the expression of stem cell markers in OSE was assessed to evaluate the impact on stemness. Alterations in the gut microbiome composition were assessed using 16S rRNA gene Long-Read sequencing and changes in the microRNA profile of granulosa cells and plasma were analyzed using qPCR. Our results demonstrated alterations in stemness markers and, a significant alteration in gut microbiome composition in DHT-induced rats compared to controls, characterized by shifts in the relative abundance of specific bacterial taxa, particularly *Akkermansia muciniphila*. Elevated levels of miR-574 and miR-378 were observed in plasma, whereas miR-21 and miR-574 showed increased expression in ovarian granulosa cells. Concurrently, increased expression of stem cell markers was observed in OSE, suggesting an enhancement of stemness in response to PCOS-like conditions. These findings imply a potential link between gut microbiome dysbiosis and increased ovarian stemness in PCOS, suggesting that the gut microbiome may contribute to ovarian dysfunction through modulation of stem cell activity. Understanding this interaction could provide novel insights into therapeutic targets in restoring ovarian function in PCOS patients.

**Keywords** PCOS, Stemness, MicroRNA, Gut Microbiome

## Introduction

Polycystic ovary syndrome (PCOS) is a complex endocrine disorder [1] associated with significant reproductive, metabolic, and psychological complications, yet its exact etiology remains unclear [2, 3]. Recent evidence suggests that PCOS may arise from a combination of genetic, hormonal, and environmental factors, contributing to disruptions in ovarian function and systemic metabolic homeostasis [4]. Despite the extensive research in the field, there are still gaps in our knowledge in some aspects including the influence of PCOS on ovarian stemness, the gut microbiome in the pathogenesis of PCOS, and microRNA profile in plasma and ovarian granulosa cells in PCOS.

<sup>†</sup>Fereshteh Esfandiarienezhad and Xiaoshu Zhan Co-first authors.

\*Correspondence:

Julang Li  
jli@uoguelph.ca  
Benjamin K. Tsang  
btsang@ohri.ca

<sup>1</sup>Inflammation and Chronic Disease Program, Ottawa Hospital Research Institute, Ottawa, ON, Canada

<sup>2</sup>Departments of Obstetrics and Gynecology & Cellular and Molecular Medicine, University of Ottawa, Ottawa, ON, Canada

<sup>3</sup>OriginElle Fertility Clinic and Women's Health Center, Ottawa, Canada

<sup>4</sup>Department of Animal Biosciences, University of Guelph, Guelph N1G 2W1, Canada

<sup>5</sup>School of Animal Science and Technology, Foshan University, Foshan, Guangdong, China

<sup>6</sup>Department of Obstetrics & Gynecology, McGill University, Montreal, Canada



© The Author(s) 2025. **Open Access** This article is licensed under a Creative Commons Attribution-NonCommercial-NoDerivatives 4.0 International License, which permits any non-commercial use, sharing, distribution and reproduction in any medium or format, as long as you give appropriate credit to the original author(s) and the source, provide a link to the Creative Commons licence, and indicate if you modified the licensed material. You do not have permission under this licence to share adapted material derived from this article or parts of it. The images or other third party material in this article are included in the article's Creative Commons licence, unless indicated otherwise in a credit line to the material. If material is not included in the article's Creative Commons licence and your intended use is not permitted by statutory regulation or exceeds the permitted use, you will need to obtain permission directly from the copyright holder. To view a copy of this licence, visit <http://creativecommons.org/licenses/by-nc-nd/4.0/>.

The ovarian surface epithelium (OSE) plays a pivotal role in folliculogenesis and ovarian function [5], OSE ruptures during each ovulation to allow the release of the oocyte and is quickly repaired [6]. Stemness properties in OSE and rapid expansion of stem cells around the wound have been suggested as the potential mechanisms in wound healing after ruptures [7]. Whether stemness in OSE changes during the normal folliculogenesis cycle has yet to be determined. Moreover, how PCOS can affect the stemness in OSE is still unknown. Here, we investigated the changes in stemness in OSE by evaluating the cells which express the well-known stem cell markers SSEA1, Oct4 and Sox2 during the estrus cycle and in a PCOS rat model.

Additionally, the gut microbiome has been linked to developing PCOS across various experimental models. For example, in DHT-induced PCOS mouse models,  $\beta$ -diversity of the gut microbiome is significantly altered, with *Bacteroides acidifaciens*—negatively associated with obesity—markedly decreased in PCOS-like mice [8]. In both human and PCOS animal models, *Bacteroides vulgatus* is significantly increased, and fecal transplantation from PCOS mice to healthy mice induces PCOS-like ovarian changes [9]. However, the variability in gut microbiome composition across different PCOS subtypes complicates model selection in PCOS research, often leading to inconsistent or unexpected results.

PCOS is a complex condition characterized by multifactorial pathogenesis involving both genetic and environmental factors. While genetic predisposition and dysregulated androgen metabolism are well-established contributors to the development of PCOS, many indirect factors have also been implicated in its pathogenesis. MicroRNAs, small non-coding RNAs that regulate gene expression, play critical roles in PCOS and its associated conditions such as insulin resistance, obesity, and hyperandrogenism [10]. Although the role of specific miRNAs has been confirmed in certain PCOS models, their expression profiles across different models and tissues remain inconsistent [10, 11]. In dihydrotestosterone (DHT)-induced PCOS rat models, miRNA expression levels have been studied in the ovarian cortex tissue [12]. However, these profiles in both plasma and granulosa cells remain largely unexplored.

We hypothesize that PCOS associates with alterations in ovarian stem cell activity, which may be linked to both circulating miRNA profiles and gut microbiome dysbiosis. This hypothesis is grounded in emerging evidence suggesting that (1) OSE stemness plays a role in tissue homeostasis [7], (2) miRNAs are key regulators of ovarian function and metabolic processes [13], and (3) imbalance of the gut microbiota composition can lead to PCOS [14]. However, these three components have not been studied together in the context of PCOS.

To address this gap, we designed the study to provide a primary insight into stemness, gut microbiome and circulation of microRNAs in DHT-induced PCOS rat model. This model has been well established in our lab and exhibits hyperandrogenism, anovulation, and metabolic alterations [12], which resemble key PCOS characteristics in humans. While, preliminary in nature, this short communication will spark future research in uncovering the role of stem cells in PCOS and how the interplay between stem cells, microbiome, and microRNA could possibly contribute to its pathophysiology by influencing ovarian function, inflammation, and metabolic processes.

## Methods

### Animal, DHT implants and cell isolation from ovary surface epithelium

All animal procedures were carried out in accordance with the Guidelines for the Care and Use of Laboratory Animals, Canadian Council on Animal Care, and were approved by the University of Ottawa Animal Care Committee (OHR1e-3708 [Replacing OHR1e-1624]-R2). Female Sprague Dawley rats (Charles River, Montreal, Canada) were maintained on 12 h cycle (light and dark) and given food and water ad libitum. Immature female rats at 20 days of age were implanted subcutaneously with silicone capsules without (control) or with DHT (DHT, Steraloids Inc., Newport, USA), as previously described [15] to continuously release 83 mg DHT/day for 28 days. Animal weight was recorded before installing the empty or DHT-loaded implants and 28 days after surgery.

Forty two female rats at 20 days of age were divided into two groups: control (implanted subcutaneously with empty silicone capsules) and DHT (implanted subcutaneously with DHT-loaded silicone capsules). Animal were sacrificed 28 days after surgery, and ovaries were collected and treated with Trypsin (5–10 min), followed by scraping of the surface epithelium with a scalpel blade. Isolated cells were stored in N<sub>2</sub> tank for subsequent analysis. Following cell isolation from the surface epithelium, ovaries were transferred to a 60 mm cell culture dish containing M199 medium. Granulosa cells, released by puncturing the large preantral follicles under a stereo-microscope, were mixed by pipetting several times and passed through a 40  $\mu$ m cell strainer for single cell collection. The cell filtrate was then centrifuged (1000 $\times$ g, 10 min at room temperature). The supernatant was discarded, and the cell pellet was resuspended in M199 medium containing 10% fetal bovine serum (FBS). The cell suspension was then plated in a 6-well culture plate and incubated at 37 °C overnight. After 24 h, the cell culture supernatant was discarded, and the cells were rinsed twice with warm PBS to remove unattached cells, such as dead cells and contaminating immune cells.

Subsequently, the granulosa cells were harvested for further miRNA detection.

### Estrus cycle assessment

Twenty mature rats were included in this experiment. Vaginal smears were prepared for each rat every morning at 7:30 AM, slides were air dried and stained with Toluidine Blue O. Estrus cycle was assessed for 3–4 days to confirm estrus cyclicity and to determine the specific stage of the estrus cycle. (Supplementary Fig. 1A). Rats were sacrificed at each stage of estrus cycle (proestrus, estrus, metestrus or diestrus), and cells were isolated from ovary surface epithelium and stored at N<sub>2</sub> for subsequent analysis. Estrous cycle assessment also was done for rats with empty implants.

### Fluorescent activated cell sorting (FACS) analysis

Due to the limited number of prospect stem cells in the ovarian surface epithelium, the isolated cells were pooled for FACS analysis. Isolated cells from control rats and DHT treated rats were pooled together respectively. Isolated cells from rats which were determined at proestrus,

and estrus stages were pooled as P + E group, as were cells from rats at metestrus and diestrus stages as M + D group because the levels of its reproductive hormones are at the high and low levels, respectively. Isolated cells were incubated with PE-conjugated SSEA1 (Sigma, at saturated concentration; 30 min, 4 °C) and fixed permeabilized using eBioscience™ Fcγ3 / Transcription Factor Staining Buffer Set (ThermoFisher Scientific, cat# 00-5523-00; as manufacture's instruction). The fixed and permeabilized cells were then incubated with FITC-conjugated Sox2 (Sigma, cat# FCMA112F at concentration suggested by manufacturer and depending on the number of cells in each group) and Oct-4 (abcam, cat# ab181557, 1 h, 37°C). Oct4 was conjugated to pacific blue, using APEX™ Antibody Labeling Kit (ThermoFisher Scientific, cat# A10478; as per manufacture's instruction). Cells were run on Beckman Coulter MoFlo XDP.

### Total RNA isolation and qRT-PCR

Total RNA from ovarian granulosa cell samples was isolated, using the Norgen Total RNA Purification Kit (Norgen Biotek, Cat#: 17200, Thorold, ON, CA) as previously

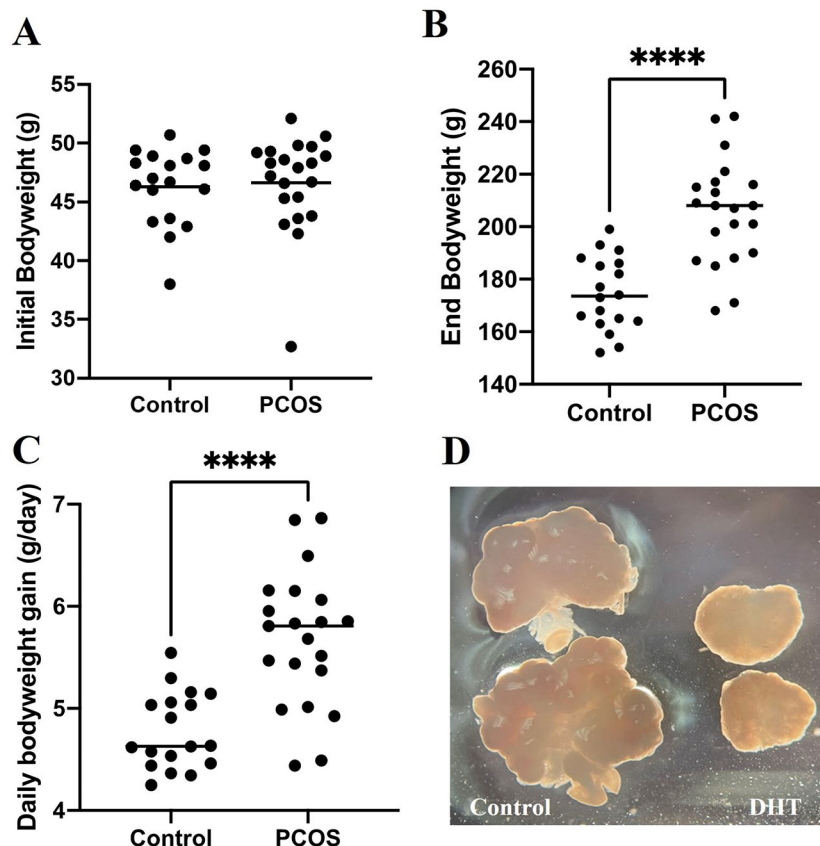


**Fig. 1** Impact of DHT Implantation on Bodyweight and Ovarian Morphology in Rats. **A**) Initial bodyweight of the rats in both groups. **B**) The end bodyweight of the rats in both groups. **C**) Daily bodyweight gain calculated for rats in each group. **D**) Representative ovarian morphology with the control group on the left and the PCOS model group on the right. Values were means  $n = 18$  (Control group) or 21 (PCOS group) rats. Statistical significance was determined using a T-test. Asterisks indicate significant differences in gene expression compared to the control group (\*\*\*\* $p < 0.0001$ )

described. Briefly, after a 24 h culture, the spent media were removed, and the cells were rinsed twice to remove dead cells. Then, 300  $\mu$ L of lysis buffer (provided by the kit) was added to each well, and the contents were pipetted up and down to ensure complete cell lysis. Total RNA was extracted according to the manufacturer's protocol. The RNA concentration and 260/280 ratio were measured using a NanoDrop 8000 (Thermo Fisher, Cat#: ND8000-GL, Waltham, MA, USA) to verify RNA quality for reverse transcription. The isolated RNA was reverse-transcribed into complementary DNA (cDNA) for miRNA detection, using the miRCURY LNA RT kit (Qiagen, Cat#: 339340, Hilden, Germany), as per manufacturer's instructions. The reaction was incubated in a thermocycler at 95 °C for 5 min, 42 °C for 60 min, and cooled to 4 °C. Prior to qPCR, the miRNA cDNA was diluted 20-fold with nuclease-free water. Quantitative PCR (qPCR) was performed using the miRCURY LNA Universal RT microRNA PCR kit (Exiqon, Cat#: 203400, Vedbaek, Denmark), in accordance with the manufacturer's protocol. miRNA-specific primers were obtained from Qiagen (Cat#: 339306, Hilden, Germany). Amplification was carried out at 95 °C for 10 min, followed by 45 cycles of 95 °C for 10 s and 60 °C for 1 min, with a ramp rate of 1.6 °C/sec, using a Bio-Rad CFX Connect Real-Time PCR System (Bio-Rad, Berkeley, CA, USA). The expression of target miRNAs was normalized to the housekeeping gene U6, and relative quantification was performed using the  $2^{-\Delta\Delta CT}$  method. The changes in gene expression were presented as fold changes relative to the control group.

#### Gut Microbiome DNA extraction 16 S rRNA sequencing

Fecal samples were collected from the colon immediately after euthanasia and subsequently shipped on dry ice to Dalhousie University (Halifax, Nova Scotia, Canada) for DNA extraction. High-throughput 16 S rRNA gene long-read sequencing was conducted on a PacBio Sequel II platform. Bioinformatic processing of the gut microbiome data was performed as previously described, with minor modifications [16]. Briefly, the raw sequence reads were subjected to standard quality-control checks and demultiplexed to separate individual samples. Chimeric sequences were identified and removed using an internal chimera detection algorithm within the Quantitative Insights into Microbial Ecology 2 (QIIME2) pipeline. The QIIME2 workflow was then employed for data cleaning, denoising, and cluster analysis. Taxonomic assignment of amplicon sequence variants (ASVs) was carried out using the SILVA database (release 132) in conjunction with the QIIME2 feature-classifier classify-sklearn function. Data visualization was facilitated by the STAMP software [17, 18]. Significant differences in predictive metagenomic pathways were assessed using Welch's t-test. All raw data

have been deposited in the Sequence Read Archive (SRA) at the National Center for Biotechnology Information (NCBI) under accession number SUB15094269.

#### Statistical analysis

Statistical analysis was performed using SAS version 9.1 (SAS Institute, Cary, NC, USA) with each rat as the experimental unit, DHT treatment as the fixed effect, and independent replicate as the random effect. Statistical significance was determined with either an ANOVA post hoc Tukey test or independent two sample *t*-test. Differences at  $p < 0.05$  were considered significant. For in vitro assays, data was analyzed with a one-way ANOVA with treatment differences determined using a GraphPad Prism software version 9.0. Data was considered significant if  $p < 0.05$ .

#### ChatGPT

We used ChatGPT to polish some paragraphs and drafting a few paragraphs of the manuscript.

## Results

### Establishment of the PCOS rat model

The initial body weights (at 20 days of age) in the control and DHT-treated groups were 46.12 g and 46.32 g, respectively, with no significant difference between the two groups. After 28 days of PCOS induction, the final body weight of DHT-implanted rats increased to 204.14 g, with an average daily weight gain of 5.692 g/day, compared to the control group's final body weight of 173.98 g and a daily weight gain of 4.78 g/day. This difference in weight gain between the groups was statistically significant (Fig. 1A-C). Additionally, ovaries collected from the control group were larger than those from the PCOS group and exhibited visible corpus lutea structures, indicating normal ovulatory function. In contrast, ovaries from DHT-treated rats were smaller, lacked visible corpus luteum, and exhibited cystic structures (Fig. 1D and Supplementary Fig. 1B), consistent with the characteristics of PCOS.

### Stemness in ovarian surface epithelium changes during estrus cycle

Based on estrus cycle assessment, OSE cells from 11 rats at proestrus or estrus stage were isolated and pooled as P+E group. In addition, OSE cells from nine rats identified at metestrus or diestrus stage were isolated and pooled as M+D group. We observed four different subpopulations of OSE stem cells in terms of SSEA1, Oct4 and Sox2 expression: (1) SSEA1 (+)/Oct4 (-)/Sox2 (-), (2) SSEA1 (+)/Oct4 (+), (3) SSEA1 (-)/Oct4 (+), (4) SSEA1 (-)/Sox2 (++)): high expression of Sox2 and SSEA1 (+)/Sox2 (+) was observed OSE stem cells in rats at all stages of estrus cycle (Fig. 2A).

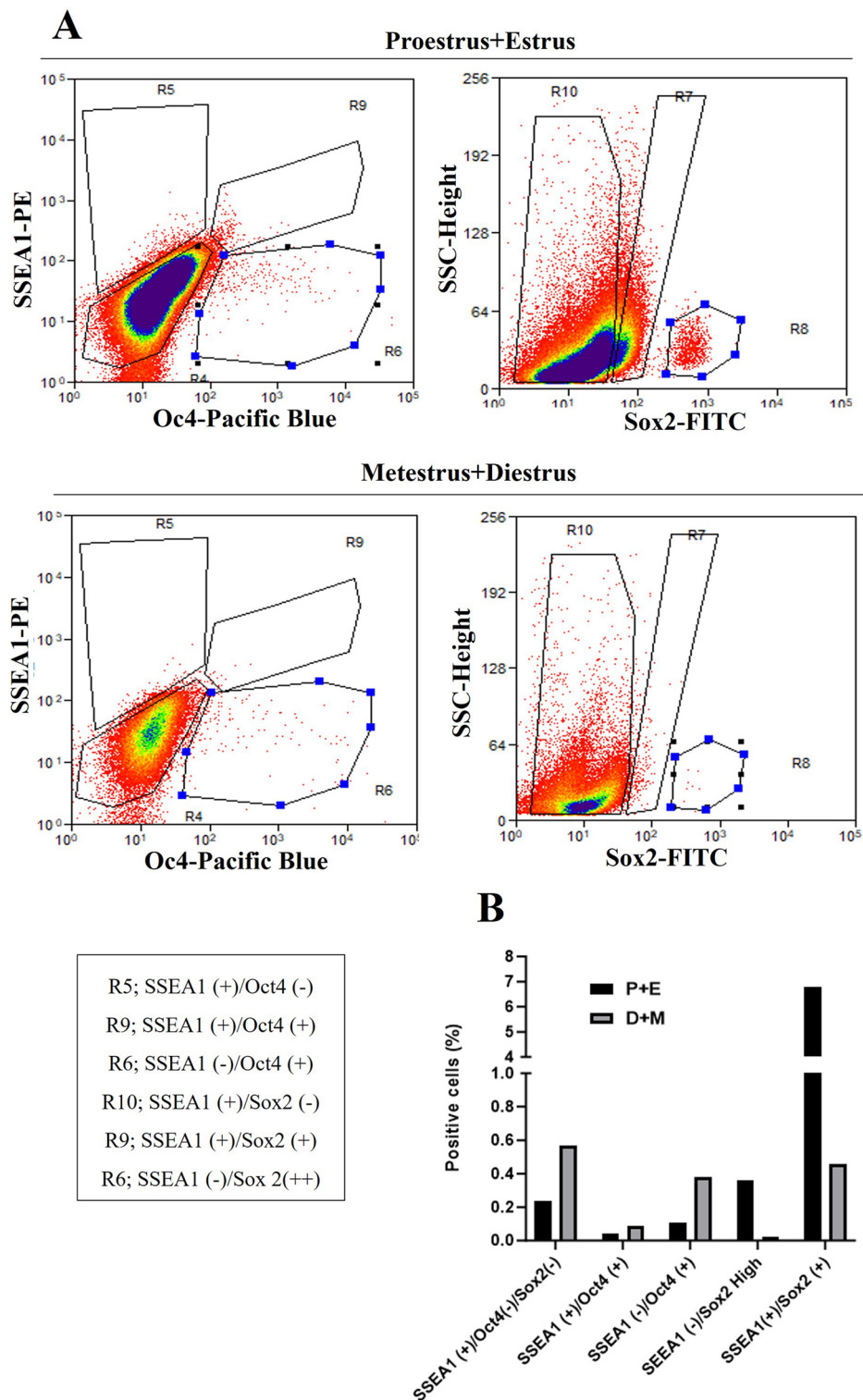


**Fig. 2** Flowcytometry analysis for stem cells marker in the ovary surface epithelium of normal cycling rats. **A**) Flowcytometry graphs for SSEA1, Oct4 and Sox2 expression in the ovary surface epithelium of rats at proestrus+estrus and metestrus+diestrus stage. **B**) Changes in stem cell subpopulations in estrus cycle in cycle phases with high level (proestrus and estrus) vs. low level of hormones (metestrus+diestrus)

The percent of cells in each subpopulation changed during cycling phases with the most alteration in the SSEA1 (+)/Sox2 (+) subpopulation from 6.8% at P+E to 0.46% at M+D, which is more than a 14-fold decrease. SSEA1 (-)/Sox2 (++) subpopulation decreased from 0.36% at P+E to 0.02% at M+D. SSEA1 (+)/Oct4 (+) subpopulation increased from 0.04% at P+E to 0.09% at M+D. The other two subpopulations increased at M+D compared to P+E; SSEA1 (+)/Oct4 (-)/Sox2 (-) from 0.24% at P+E to 0.57% at M+D, SSEA1 (-)/Oct4 (+) from 0.11% at P+E to 0.38% at M+D (Fig. 2B).

### Stemness in ovary surface epithelium is affected in PCOS ovaries

Isolated cells from all 21 rats with DHT implants were pooled together as a PCOS group. Estrus cycle was assessed for rats in control group for two purposes: (1) to confirm that they are cycling and (2) to collect the ovaries at metestrus or diestrus stages when gonadotropic hormone levels are low. Two rats in the control group did not have regular estrus cycle as they did not exhibit the proestrus, estrus, metestrus and diestrus stages: rat # 14 (proestrus stage at the first day of assessment, two days at estrus and then two more days at proestrus); Rat # 27 (late diestrus stages at the day of assessment and then cycling between proestrus and estrus stages only for four days). These two animals were excluded from the study. One of the rats did not recover after surgery and so there were 18 rats in the control group at the end of the experiment; isolated cells from the ovary surface epithelium of these 18 rats were pooled together as a control group and cells isolated from OSE of 21 rats with DHT implants were pooled together as PCOS group for FACS analysis.

Among the evaluated subpopulations, SSEA1 (+)/Oct4 (-)/Sox2 (-) and SSEA1 (-)/Sox2 (++) were increased in PCOS ovaries by more than 2-folds. SSEA1 (+)/Oct4 (-)/Sox2 (-) subpopulation was 0.82% in PCOS ovaries compared to 0.32% in control, which showed a 2.5-fold increase. SSEA1 (-)/Sox2 (++) is 0.19% in PCOS ovaries comparing to 0.07% in control which showed 2.7-fold increase. There was also a slight increase in SSEA1 (+)/Sox2 (+) from 4.97% in control to 6.02% in PCOS ovaries. We did not observed differences in SSEA1 (+)/Oct4 (+) and SSEA1 (-)/Oct4 (+) subpopulations in PCOS ovaries when compared to control (Fig. 3A&B).

### MiRNA levels in plasma and ovarian granulosa cells in a DHT-induced PCOS rat model

MiR-21, -29b, -195, -378, and -574 are known to regulate ovarian function and are associated with ovarian-related diseases in various species [17–19]. To investigate whether these miRNAs are altered in the DHT-induced PCOS model, their levels was analyzed in both plasma and ovarian granulosa cells. The results revealed that

miR-21 and miR-574 in ovarian granulosa cells were significantly upregulated in the PCOS group ( $p < 0.05$ ), while miR-29b, miR-195, and miR-378 showed no significant differences between the groups (Fig. 4A). In contrast, the miRNA expression profile in plasma differed from that in granulosa cells. In the plasma, miR-378 and miR-574 levels were significantly elevated in the DHT-induced PCOS rats ( $p < 0.05$ ), whereas miR-21, miR-29b, and miR-195 exhibited no significant differences in their levels between the two groups (Fig. 4B).

### Gut Microbiome composition altered in DHT-induced PCOS rat model

Next, we analyzed the dynamics of the gut microbiome in both the control and DHT-treated groups by sequencing the 16S rRNA gene region. Overall, no significant changes in alpha-diversity were observed between the two groups, as indicated by the Shannon richness index (Figure. 5 A). To assess  $\beta$ -diversity (between-sample diversity), we used unweighted and weighted UniFrac distances. The PCoA plot based on the unweighted UniFrac distance demonstrated a clear separation between the control and DHT-treated groups (Fig. 5B&C). To further investigate whether DHT treatment affects the relative abundance of gut microbiota,  $\beta$ -diversity within each group was analyzed, and the top 20 most abundant bacterial taxa were plotted at level 6 (Fig. 6A) and level 7 (Fig. 6B). At level 6, the control group was primarily dominated by *Lactobacillus*, followed by *Akkermansia* and *Muribaculaceae*, whereas in the DHT-treated group, *Muribaculaceae* and *Romboutsia* were predominant. At level 7, the top four most abundant species in both groups were *Lactobacillus intestinalis*, *Akkermansia muciniphila*, *Romboutsia ilealis*, and *Lactobacillus reuteri*. STAMP analysis identified significant differences in nine bacterial species between the two groups ( $p < 0.05$ ), with *Parabacteroides distasonis*, *Ruminococcus*, and *Akkermansia muciniphila* showing the most pronounced reductions in the DHT-treated group (Fig. 7A-D).

### Discussion

This study aimed to investigate the changes in stemness markers in the OSE, alterations in miRNA expression in granulosa cells and plasma, and shifts in gut microbiome composition in a DHT-induced rat model of PCOS. By investigating these three components, we provided foundational information on the complex interplay between stem cells, microRNAs, and the microbiome in the pathophysiology of PCOS.

The DHT-induced rat model of PCOS is a well-established and widely used model for studying the pathophysiology of PCOS, including its reproductive and metabolic characteristics. Previous studies, including those from our laboratory, have demonstrated that continuous DHT

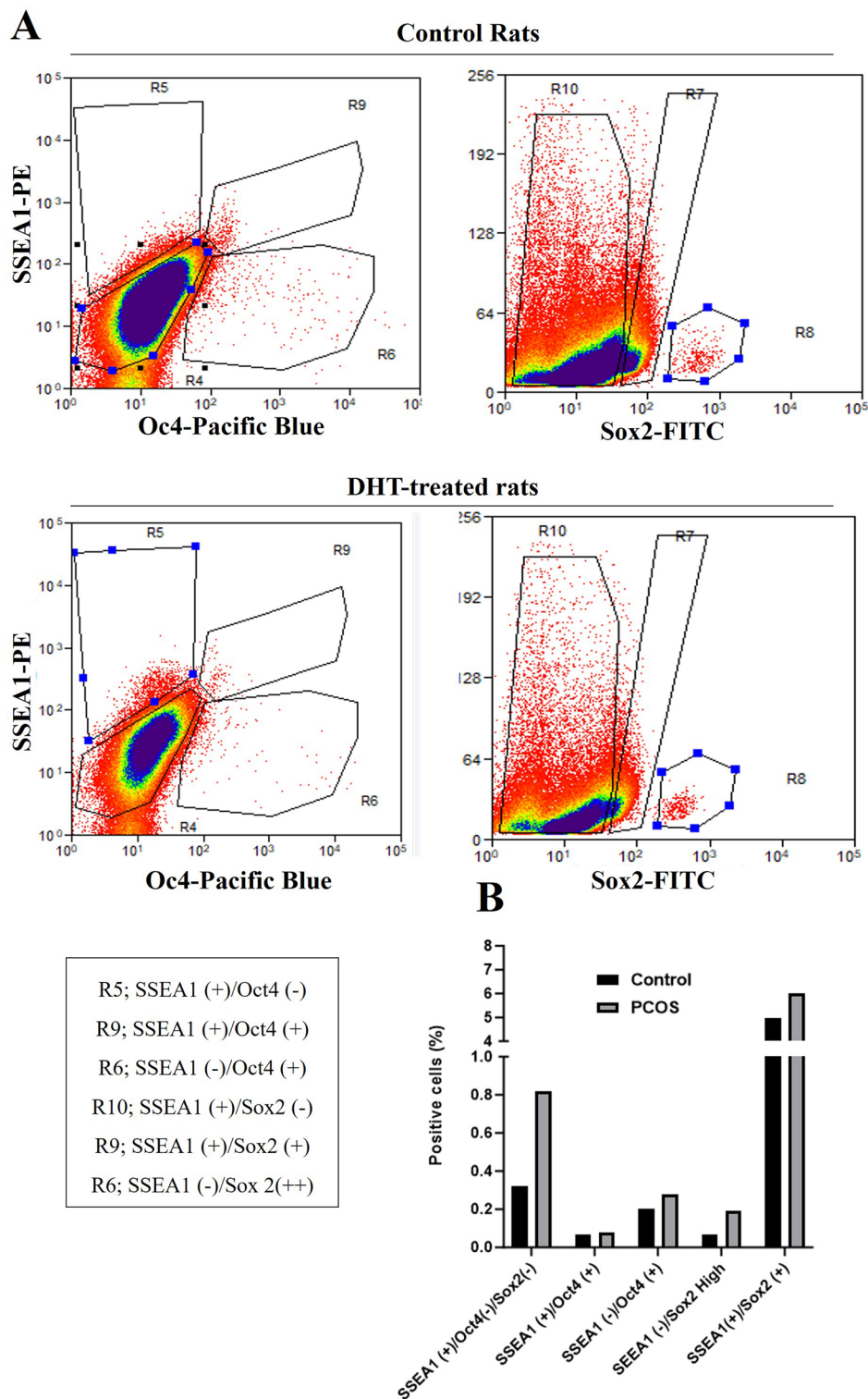


**Fig. 3** Flowcytometry analysis for stem cells marker in the ovary surface epithelium of control and PCOS rats. **A**) Flowcytometry graphs for SSEA1, Oct4 and Sox2 expression in the ovary surface epithelium of control and DHT-treated rats. **B**) Changes in stem cell subpopulations in control vs. DHT-treated rats

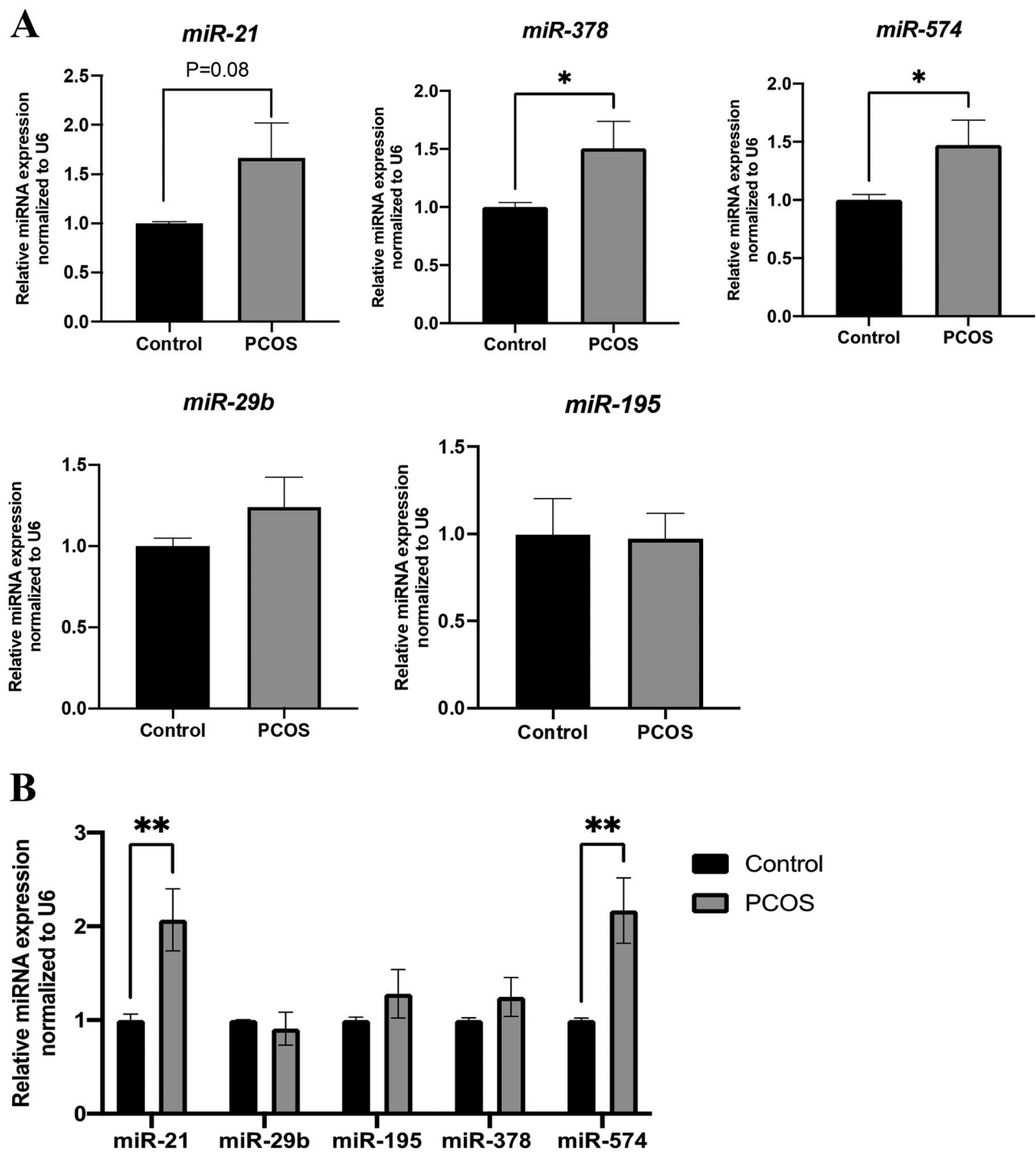


**Fig. 4** DHT implantation alters the miRNAs levels in both plasma and ovarian granulosa cells of the rats in both groups. **A)** Specific microRNA levels in the plasma of the rats in both groups. **B)** Specific microRNA levels in the ovarian granulosa cells of the rats in both groups. For the plasma samples, the data represent means for  $n = 12$  samples, with 4 rats randomly selected from each group for each of three replicates. For the granulosa cell samples, the data represent means for  $n = 4$  (control group) and  $n = 5$  (PCOS group) samples, with granulosa cells pooled from 4–5 rats per sample. Asterisks denote statistically significant differences in gene expression relative to the control group ( $*p < 0.05$ ,  $**p < 0.01$ )

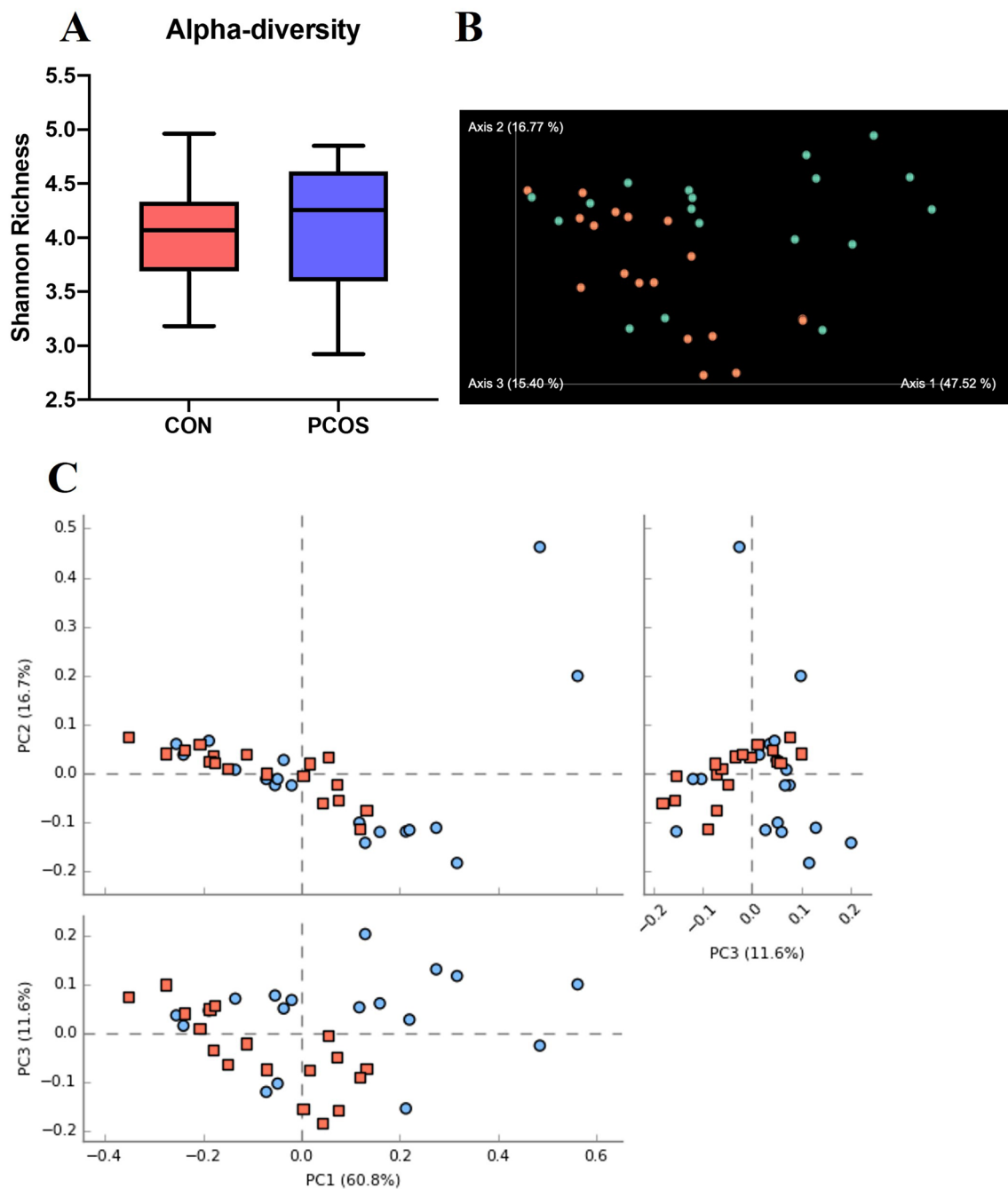


**Fig. 5** Boxplot of alpha diversity (Shannon index) and beta-diversity of the gut microbiome in both Control and PCOS rats. **A)** Alpha diversity indices, represented by the Shannon index, quantify the species richness and evenness within the microbiota from a designated number of individual samples. A higher index value indicates greater diversity within the sequenced microbial community. **B)** Principal Coordinates Analysis (PCoA) based on unweighted and weighted UniFrac, as well as Bray-Curtis distances, evaluates the similarity between microbiome samples from the two groups. Samples that cluster more closely in the plot are more similar in microbial composition than those that are further apart. Data represent averages from 18 rats per group. Statistical significance of differences was determined using an independent two-sample t-test

exposure leads to hyperandrogenism, disrupted estrous cycles, and polycystic ovarian morphology and no corpora lutea. This model also exhibits metabolic disturbances, decreased insulin sensitivity, altered adipokine (leptin and chemerin) concentrations in DHT treated

rats [12, 19–22]. These metabolic abnormalities align with the body weight differences observed in our study, where DHT-implanted rats exhibited significantly higher body weight gain compared to controls (Fig. 1A–C), further supporting the metabolic relevance of this model.

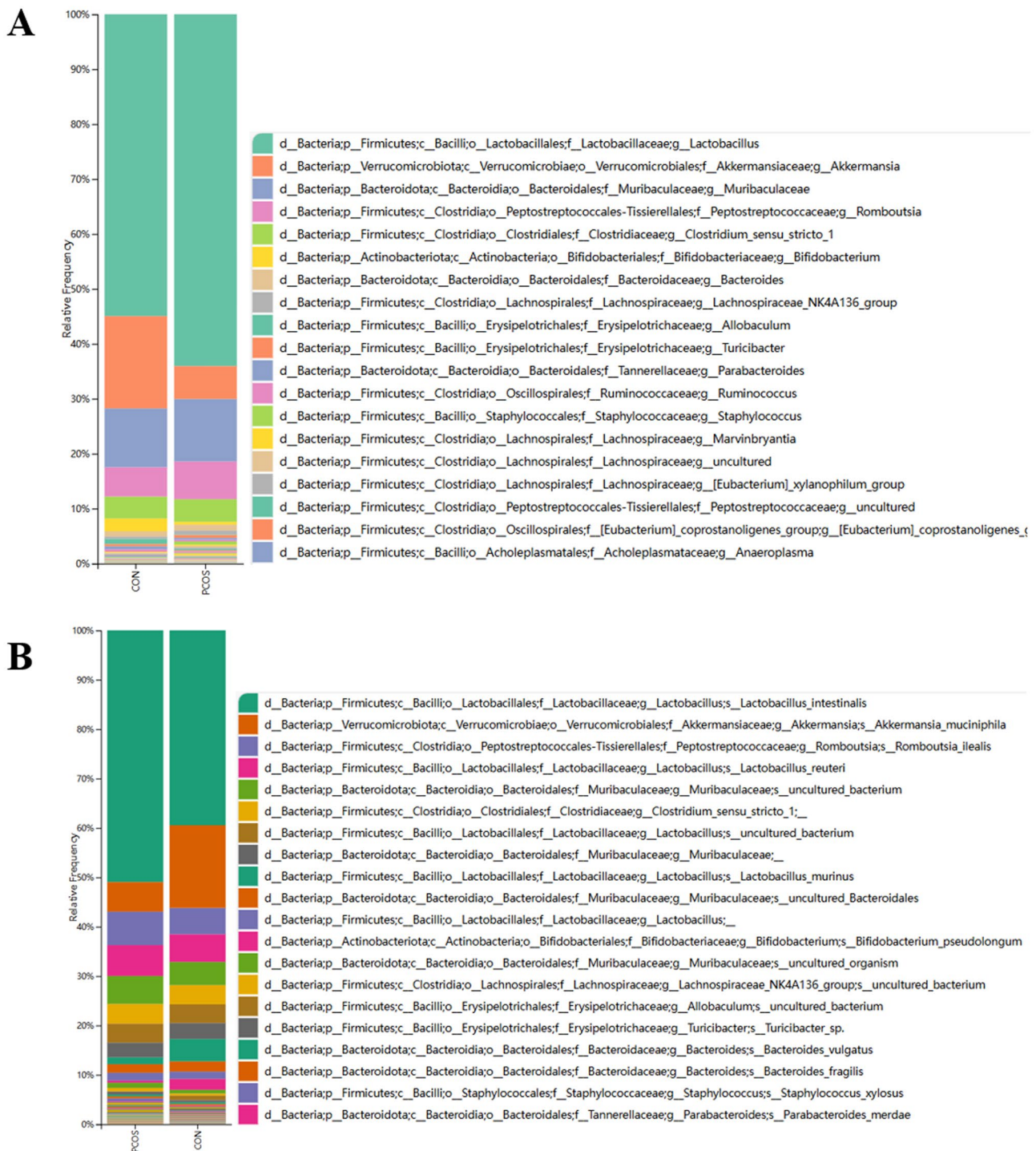


**Fig. 6** Bar plot of microbial composition at the phylum and genus level. **A**) Bar plot of microbial composition at the phylum level (level 6). **B**) Bar plot of microbial composition at the genus level (level 7)

Given its well-characterized hormonal, ovarian, and metabolic alterations, this model provides a robust system for investigating the interplay between ovarian stem cell dynamics, miRNA expression, and gut microbiome composition in PCOS.

The changes in stemness markers in the OSE during different stages of the estrus cycle and under PCOS conditions revealed interesting findings. The decrease in stem cell subpopulations expressing SSEA1 (+)/Sox2 (+) and SSEA1 (-)/Sox2 (++) during the metestrus and diestrus stages (M + D) suggests that stem cell activity in

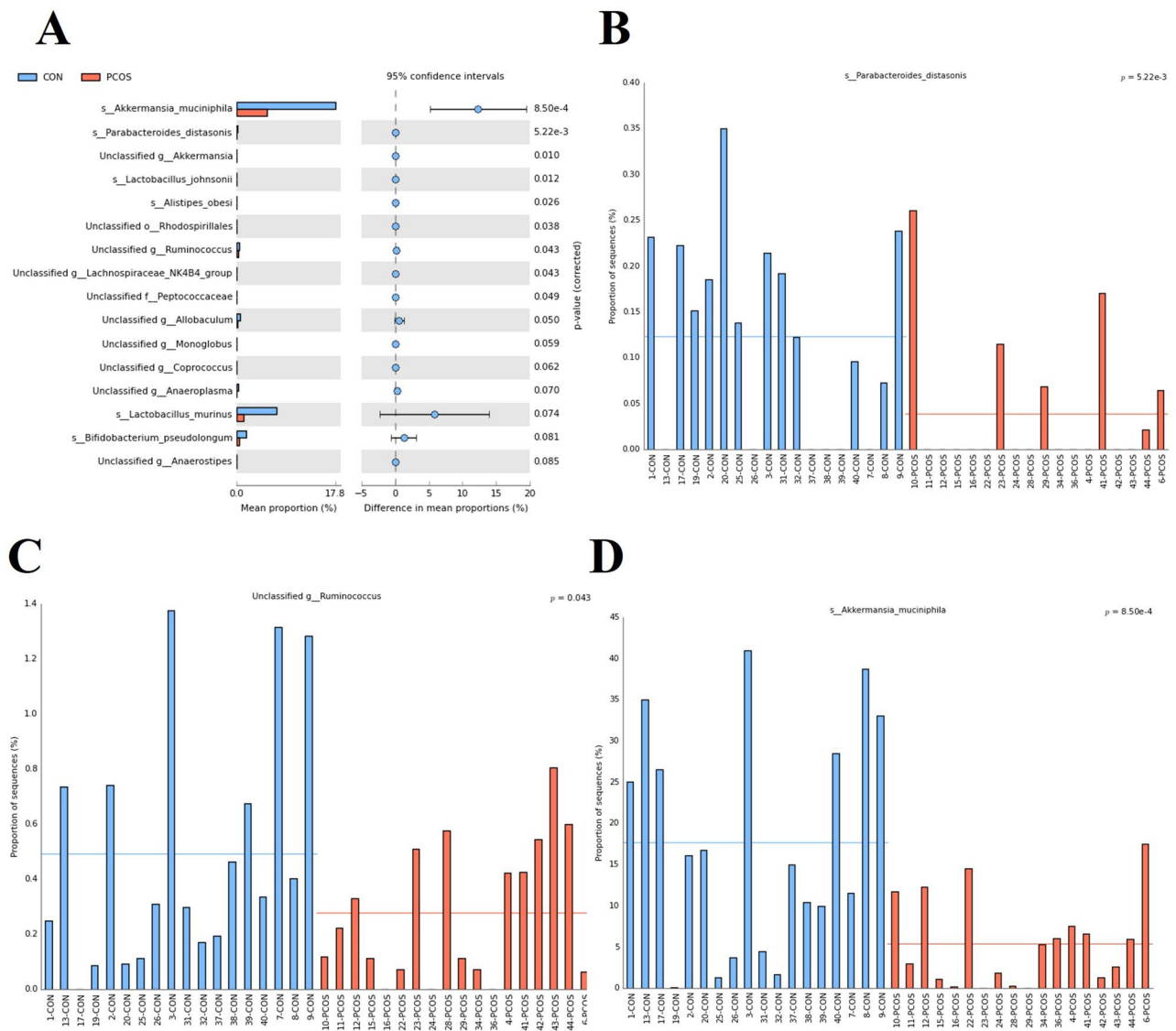


**Fig. 7** Fecal bacteria abundance at the species level by STAMP analysis. **A**) Comparison of gut microbiota between the controls and PCOS rats by STAMP analysis at the species level with the p value less than 0.1. Relative abundance of *Parabacteroides Distasonis* (**B**), *Ruminococcus* (**C**), *Akkermansia Muciniphila* (**D**) in both Control group (Blue) and PCOS group (Red)

the OSE is influenced by hormonal fluctuations, possibly regulated by gonadotropins that are higher during the proestrus and estrus (P + E) stages. In line with our finding, ecdysteroids (i.e., a type of steroid hormone found in arthropods) is essential in *Drosophila* ovary for female germline stem cell proliferation and maintenance [23]. Moreover, hormones control stem cell proliferation and differentiation in other organs such as hematopoietic system, intestine and mammary gland [24]. These dynamic changes in stem cell subpopulations during the estrus cycle suggest their importance in supporting the cyclical nature of follicular development and ovulation. Whether this indeed is the case in the mammalian ovary remains to be determined.

In the DHT-induced PCOS model, we observed higher levels in two stem cell subpopulations—SSEA1 (+)/Oct4 (-)/Sox2 (-) and SSEA1 (-)/Sox2 (++)—compared to the control group. This increase in stemness in the OSE under PCOS conditions suggests that androgen excess may stimulate the expansion or differentiation of specific stem cell populations. SSEA1, Oct4, and Sox2 are well-known key markers of stemness [25]; Oct4 and Sox2 are essential transcription factors for the maintenance of pluripotency and self-renewal in stem cells [26, 27], while SSEA1 is expressed in early-stage undifferentiated cells [28, 29]. As stem cells differentiate, the expression of these markers typically decreases or shifts, with SSEA1 [28] and Oct4 [30] downregulated during differentiation, while Sox2 may remain elevated in progenitor or partially

differentiated cells [31], showing a dynamic balance between stemness and differentiation. Our observation of increase in the SSEA1 (+)/Oct4 (-)/Sox2 (-) and SSEA1 (-)/Sox2 (++) subpopulations in the PCOS model could indicate altered stemness under pathological conditions. The expansion of these subpopulations may suggest that in PCOS, there is a disruption in the normal balance between stemness and differentiation, possibly favoring a progenitor-like state (high Sox2 expression without Oct4 and SSEA1) and more lineage-committed population (SSEA1 positive without Oct4 and Sox2).

The enrichment of SSEA1(+)/Oct4(-)/Sox2(-) cells could reflect a tendency toward the differentiation of stem cells into theca progenitor cells, as SSEA1 expression without Sox2 or Oct4 aligns with a more lineage-committed state. Conversely, the SSEA1(-)/Sox2(++) population, indicative of a progenitor-like state, may highlight disrupted or incomplete differentiation into granulosa cell populations. This imbalance in differentiation could potentially contribute to the disrupted folliculogenesis and may be a consequence of hormonal dysregulation observed in PCOS. Which of these mechanisms - favoring stem cell differentiation toward theca progenitor cells (SSEA1 without Sox2 and Oct4) or disrupted differentiation toward granulosa cells (progenitor-like state) - is predominantly driving the pathophysiology in PCOS remains to be determined and requires further investigation. Furthermore, the increased presence of these stem-like cells may also indicate a compensatory mechanism where the ovary attempts to maintain or regenerate tissue in response to hormonal imbalances.

The gut microbiome plays a critical role in regulating metabolism by influencing energy homeostasis [32], insulin sensitivity, and inflammation [33], all of which are key factors in metabolic disorders like PCOS. Gut microbiome dysbiosis has been observed in both DHEA-induced PCOS mouse models and in women with PCOS. Specifically, *Bacteroides vulgatus* was found to be significantly decreased in both groups. Furthermore, transplanting *Bacteroides vulgatus* into healthy mice induced a PCOS-like phenotype [9]. In contrast to these models, our study found no difference in *Bacteroides vulgatus* levels between the control and PCOS rat groups. Whether this is due to species differences is unclear at this point. Interestingly, significant reductions were observed in *Akkermansia muciniphila*, *Parabacteroides distasonis*, *Ruminococcus*, and *Lactobacillus johnsonii* in the PCOS model, with the most pronounced decrease noted in *Akkermansia muciniphila*. Although no evidence has established a causal relationship between PCOS and *Akkermansia muciniphila*, numerous reports have highlighted associations between this bacterium and conditions such as obesity, insulin resistance, and diabetes [34, 35]. Moreover, supplementation with *Akkermansia*

*muciniphila* has been shown to improve insulin sensitivity and inflammatory markers in overweight women [36]. However, the underlying mechanisms of these effects remain largely unexplored. Our findings may suggest a potential relationship between gut microbiome alterations and stemness in the OSE. Specifically, the alteration in gut microbiome composition observed in the DHT-induced rat model of PCOS may influence the ovarian microenvironment by mediating changes in hormonal and metabolic signaling pathways, potentially affecting stem cell activity [37]. This highlights the potential interplay between gut microbiome dysbiosis and ovarian stem cell behavior, suggesting that metabolic disturbances in PCOS may be mediated in part by changes in the microbiome that impact stem cell function and ovarian health. However, further study is required to determine whether changes in gut microbiome and stemness in the ovary in PCOS condition are parallel changes or associated.

MiRNAs have garnered significant attention in PCOS research over the past several years, though their expression profiles vary across different subtypes of PCOS. In this study, we examined several miRNAs known to regulate ovarian function, including miR-21, miR-29b, miR-195, miR-378, and miR-574. Notably, miR-21 was found to be elevated in granulosa cells (GCs) of DHT-induced PCOS rats, which aligns well with previous findings in hyperandrogenic PCOS patients [38]. MiR-21 is known to play an important role in regulating ovarian function [39, 40]. Furthermore, functional studies have shown that miR-21 from adipose-derived mesenchymal stem cells can enhance hepatic metabolism, potentially improving metabolic dysfunction in PCOS [10]. However, in another study using a mouse model, genetic ablation of miR-21 attenuated androgen-induced increases in body weight and lean mass, and reversed the upregulation of thermogenic genes in brown adipose tissue caused by androgen treatment [41]. These contradictory findings suggest that miR-21 could serve as a potential diagnostic marker for certain PCOS subtypes, but further functional studies are required to establish its causal role in DHT-induced PCOS. Additionally, miR-574 was found to be significantly elevated in both GCs and plasma, marking the first report of its involvement in PCOS.

Previous research has shown that miR-574 suppresses oocyte maturation by targeting hyaluronan synthase 2 in porcine cumulus cells and is positively correlated with estradiol production in porcine granulosa cells. Based on this, it can be hypothesized that the elevated levels of miR-574 in our hyperandrogenic PCOS model may reflect a compensatory mechanism to convert excess androgens to estradiol. However, elevated miR-574 levels could impair oocyte development, contributing to the anovulatory phenotype observed in this model. MiRNA-378 is another miRNA the roles of which in the

ovary have been well studied [42]. In the current study, miR-378 was found to be upregulated in the plasma of DHT-induced rats. Consistent with our findings, previous studies also reported elevated miR-378 levels in the follicular fluid of women with PCOS [43]. Overexpression of miR-378 in porcine ovarian cumulus cells has been shown to impair cumulus expansion and downregulate genes essential for this process (e.g., HAS2, PTGS2), as well as oocyte maturation [42]. Overall, the differential expression of miRNAs between granulosa cells and plasma highlights the complexity of regulatory networks involved in PCOS pathogenesis. This suggests that specific miRNA signatures may play distinct roles in different PCOS subtypes, warranting further investigation.

MicroRNAs also play important role in regulating stem cell biology which can be associated with our finding about altered stemness in PCOS. For instance, miR-21, regulate hematopoietic stem cell (HSC) homeostasis [44] and bone marrow mesenchymal stem cell (BMMSC) immunoregulatory functions [45]. Additionally, miR-378 has been shown to enhance stem cell properties in chronic myeloid leukemia cells [46] and regulate neural stem cell proliferation and differentiation. These evidence raise the possibility that the dysregulated expression of miRNAs such as miR-21 and miR-378 in PCOS granulosa cells and plasma could contributed to altered stemness in PCOS in our study. This contribution might lead to disrupt the balance between stemness and differentiation, as we observed disturbed stem cells homeostasis in PCOS rat model.

Our findings suggest that there may be a complex interplay between ovarian stem cell activity, miRNA expression, and gut microbiome composition in PCOS. We observed that the percentage of OSE stem cell subpopulations varies across the estrous cycle, indicating a potential role for hormonal regulation in maintaining stemness. In the DHT-induced PCOS model, OSE stem cell subpopulations were altered, potentially disrupting the balance between differentiation and renewal, which may contribute to impaired folliculogenesis. Additionally, dysregulated miRNA expression in granulosa cells and plasma, particularly miR-21, miR-574, and miR-378, suggests a regulatory role in ovarian function, metabolism, and inflammation. Changes in the gut microbiome, including a reduction in *Akkermansia muciniphila*, may contribute to metabolic disturbances and systemic inflammation, possibly affecting ovarian microenvironments. By integrating these findings, we propose that gut microbiome alterations and miRNA dysregulation may influence ovarian stem cell dynamics, ultimately affecting ovarian function and PCOS pathology. This potential interplay requires further investigation to determine whether targeting these factors could offer novel therapeutic strategies for PCOS.

## Conclusion

In conclusion, this study represents a series of foundational exploration on stem cell properties in the ovary surface epithelium (OSE), circulating and granulosa cell miRNA profiles, and gut microbiome composition in a DHT-induced rat model of polycystic ovary syndrome (PCOS). The observed changes in OSE stemness during different estrus cycle stages and the increased stem cell populations under PCOS conditions suggest that hormonal regulation and androgen excess may influence stem cell activity, potentially contributing to the disrupted ovarian morphology in PCOS. The shift in gut microbiome composition may suggest a link between androgen excess and microbial dynamics, suggesting that microbiome alterations may contribute to PCOS pathophysiology. Moreover, the altered expression of miRNAs, such as miR-21, miR-574, and miR-378, in granulosa cells and plasma highlights their potential role in modulating ovarian function and metabolic dysregulation associated with PCOS. Alternatively, these expression patterns may represent secondary effects stemming from the pathophysiological conditions of PCOS. Collectively, these findings underscore the complex interplay between stem cells, miRNAs, and the microbiome in PCOS and paves the way for future studies in the elucidation of the underlying mechanisms of this multifactorial disorder and in the identification of novel therapeutic targets.

## Supplementary Information

The online version contains supplementary material available at <https://doi.org/10.1186/s13048-025-01648-9>.

Supplementary Material 1: Supplementary Figure. A) Estrus cycle assessment Toluidine Blue O staining B) Ovary size in control vs. DHT treated rat. The size of ovary is reduced in DHT-treated rats.

## Acknowledgements

The authors would like to acknowledge the assistance of Fernand Ortiz at the OHRI-Flow Cytometry Core Facility, RRID: SCR\_023349. Authors would also like to thank the at animal care and veterinary service staff at uOttawa for their extraordinary support, particularly Jennifer Andrusiak, Anthony Carter, Roxanne Cote and Courtney Reeks.

## Author contributions

FE, XZ BKT, and JL designed the experiments; FE and XZ performed the experiments and analyzed experimental data, FE and XZ prepared the manuscript with input from BKT, JL and SLT. All authors reviewed and revised manuscript; BKT, JL and SLT provided financial support for the project. The authors read and approved the final manuscript.

## Funding

This work was supported by grant from the Canadian Institutes of Health Research (to BKT). Postdoctoral fellowships from the Mathematics of Information Technology and Complex Systems (Mitacs; to FE) and Montreal Reproductive and Regenerative Foundation funding contribution to MITACS fellowship (to FE). Canada First Research Excellence Fund (CFREF) and Food From Thought (to JLi); Natural Sciences and Engineering Research Council of Canada (NSERC to JLi).

### Data availability

The datasets used and/or analysed during the current study are available from the corresponding author on reasonable request. All raw data have been deposited in the Sequence Read Archive (SRA) at the National Center for Biotechnology Information (NCBI) under accession number SUB15094269.

### Declarations

#### Ethics approval and consent to participate

All animal procedures were carried out in accordance with the Guidelines for the Care and Use of Laboratory Animals, Canadian Council on Animal Care, and were approved by the University of Ottawa Animal Care Committee (OHRle-3708 [Replacing OHRle-1624]-R2).

#### Consent for publication

This manuscript does not contain any individual person's data in any form.

#### Competing interests

Benjamin K Tsang is an Editor-in-Chief, Julang Li is an Associate Editor, and Fereshteh Esfandiariñezhad is a member of the Editorial Board of the *Journal of Ovarian Research*. All decisions on this manuscript were made by another senior editor. The author(s) declare that they have no other competing interests.

Received: 21 December 2024 / Accepted: 15 March 2025

Published online: 01 April 2025

### References

- Singh S, Pal N, Shubham S, Sarma DK, Verma V, Marotta F, et al. Polycystic ovary syndrome: etiology, current management, and future therapeutics. *J Clin Med*. 2023;12:1454.
- Sanchez-Garrido MA, Tena-Sempere M. Metabolic dysfunction in polycystic ovary syndrome: pathogenic role of androgen excess and potential therapeutic strategies. *Mol Metab*. 2020;35:100937.
- Che Y, Yu J, Li Y-S, Zhu Y-C, Tao T. Polycystic ovary syndrome: challenges and possible solutions. *J Clin Med*. 2023;12:1500.
- Kumar R, Minerva S, Shah R, Bhat A, Verma S, Chander G et al. Role of genetic, environmental, and hormonal factors in the progression of PCOS: A review. *J Reprod Health Med*. 2022;3.
- Lai D, Xu M, Zhang Q, Chen Y, Li T, Wang Q, et al. Identification and characterization of epithelial cells derived from human ovarian follicular fluid. *Stem Cell Res Ther*. 2015;6:13.
- Carter LE, Cook DP, McCloskey CW, Grondin MA, Landry DA, Dang T, et al. Transcriptional heterogeneity of stemness phenotypes in the ovarian epithelium. *Commun Biol*. 2021;4:1–11.
- Wang J, Liu C, He L, Xie Z, Bai L, Yu W et al. Selective YAP activation in Procr cells is essential for ovarian stem/progenitor expansion and epithelium repair. Postovit L-M, Azziz R, editors. *eLife*. 2022;11:e75449.
- Rodriguez Paris V, Wong XYD, Solon-Biet SM, Edwards MC, Aflatounian A, Gilchrist RB et al. The interplay between PCOS pathology and diet on gut microbiota in a mouse model. *Gut Microbes*. 14:2085961.
- Qi X, Yun C, Sun L, Xia J, Wu Q, Wang Y, et al. Gut microbiota–bile acid–interleukin-22 axis orchestrates polycystic ovary syndrome. *Nat Med*. 2019;25:1225–33.
- Cao M, Zhao Y, Chen T, Zhao Z, Zhang B, Yuan C, et al. Adipose mesenchymal stem cell-derived Exosomal MicroRNAs ameliorate polycystic ovary syndrome by protecting against metabolic disturbances. *Biomaterials*. 2022;288:121739.
- Cao J, Huo P, Cui K, Wei H, Cao J, Wang J, et al. Follicular fluid-derived Exosomal miR-143-3p/miR-155-5p regulate follicular dysplasia by modulating Glycolysis in granulosa cells in polycystic ovary syndrome. *Cell Commun Signal*. 2022;20:61.
- Hossain MM, Cao M, Wang Q, Kim JY, Schellander K, Tesfaye D, et al. Altered expression of MiRNAs in a dihydrotestosterone-induced rat PCOS model. *J Ovarian Res*. 2013;6:36.
- Wang Y, Wang J, Li Q, Xuan R, Guo Y, He P, et al. Characterization of MicroRNA expression profiles in the ovarian tissue of goats during the sexual maturity period. *J Ovarian Res*. 2023;16:234.
- Qi X, Yun C, Pang Y, Qiao J. The impact of the gut microbiota on the reproductive and metabolic endocrine system. *Gut Microbes*. 13:1894070.
- Salehi R, Asare-Werehene M, Wyse BA, Abedini A, Pan B, Gutsol A, et al. Granulosa cell-derived miR-379-5p regulates macrophage polarization in polycystic ovarian syndrome. *Front Immunol*. 2023;14:1104550.
- Zhan X, Fletcher L, Huyben D, Cai H, Dingle S, Qi N, et al. Choline supplementation regulates gut Microbiome diversity, gut epithelial activity, and the cytokine gene expression in gilts. *Front Nutr*. 2023;10:1101519.
- Parks DH, Beiko RG. Identifying biologically relevant differences between metagenomic communities. *Bioinformatics*. 2010;26:715–21.
- Parks DH, Tyson GW, Hugenholtz P, Beiko RG. STAMP: statistical analysis of taxonomic and functional profiles. *Bioinformatics*. 2014;30:3123–4.
- Kim JY, Xue K, Cao M, Wang Q, Liu J-Y, Leader A, et al. Chemerin suppresses ovarian follicular development and its potential involvement in follicular arrest in rats treated chronically with dihydrotestosterone. *Endocrinology*. 2013;154:2912–23.
- Mannerås L, Cajander S, Holmång A, Seleskovic Z, Lystig T, Lönn M, et al. A new rat model exhibiting both ovarian and metabolic characteristics of polycystic ovary syndrome. *Endocrinology*. 2007;148:3781–91.
- Salehi R, Mazier HL, Nivet A-L, Reunov AA, Lima P, Wang Q, et al. Ovarian mitochondrial dynamics and cell fate regulation in an androgen-induced rat model of polycystic ovarian syndrome. *Sci Rep*. 2020;10:1021.
- Lim JJ, Lima PDA, Salehi R, Lee DR, Tsang BK. Regulation of androgen receptor signaling by ubiquitination during folliculogenesis and its possible dysregulation in polycystic ovarian syndrome. *Sci Rep*. 2017;7:10272.
- Yoshinari Y, Kurogi Y, Ameku T, Niwa R. Endocrine regulation of female germline stem cells in the fruit fly *Drosophila melanogaster*. *Curr Opin Insect Sci*. 2019;31:14–9.
- Gancz D, Gilboa L. Hormonal control of stem cell systems. *Annu Rev Cell Dev Biol*. 2013;29:137–62.
- Hadjimichael C, Chanoumidou K, Papadopoulou N, Arampatzis P, Papamatheakis J, Kretsovali A. Common stemness regulators of embryonic and cancer stem cells. *World J Stem Cells*. 2015;7:1150.
- Rizzino A. The Sox2-Oct4 connection: critical players in a much larger interdependent network integrated at multiple levels. *Stem Cells*. 2013;31:1033.
- Zhang S, Cui W. Sox2, a key factor in the regulation of pluripotency and neural differentiation. *World J Stem Cells*. 2014;6:305.
- Cui L, Johkura K, Yue F, Ogiwara N, Okouchi Y, Asanuma K, et al. Spatial distribution and initial changes of SSEA-1 and other cell Adhesion-related molecules on mouse embryonic stem cells before and during differentiation. *J Histochem Cytochem*. 2004;52:1447–57.
- Choi S-J, Shim H, Anderson GB. Short communication: lack of Stage-Specific embryonic Antigen-1 expression by bovine embryos and primordial germ cells. *J Dairy Sci*. 1999;82:516–9.
- Liedtke S, Enczmann J, Waclawczyk S, Wernet P, Kögler G. Oct4 and its pseudogenes confuse stem cell research. *Cell Stem Cell*. 2007;1:364–6.
- Graham W, Khudyakov J, Ellis P, Pevny L. SOX2 functions to maintain neural progenitor identity. *Neuron*. 2003;39:749–65.
- Fujisaka S, Watanabe Y, Tobe K. The gut microbiome: a core regulator of metabolism. 2023.
- Semo D, Reinecke H, Godfrey R. Gut Microbiome regulates inflammation and insulin resistance: a novel therapeutic target to improve insulin sensitivity. *Signal Transduct Target Ther*. 2024;9:35.
- Zhai Q, Feng S, Arjan N, Chen W. A next generation probiotic, *Akkermansia muciniphila*. *Crit Rev Food Sci Nutr*. 2019;59:3227–36.
- Liu E, Ji X, Zhou K. *Akkermansia muciniphila* for the prevention of type 2 diabetes and obesity: A Meta-Analysis of animal studies. *Nutrients*. 2024;16:3440.
- Depommier C, Everard A, Duart C, Plovier H, Van Hul M, Vieira-Silva S, et al. Supplementation with *Akkermansia muciniphila* in overweight and obese human volunteers: a proof-of-concept exploratory study. *Nat Med*. 2019;25:1096–103.
- Huang F, Cao Y, Liang J, Tang R, Wu S, Zhang P, et al. The influence of the gut Microbiome on ovarian aging. *Gut Microbes*. 2024;16:2295394.
- Naji M, Aleyasin A, Nekoonam S, Arefian E, Mahdian R, Amidi F. Differential expression of miR-93 and miR-21 in granulosa cells and follicular fluid of polycystic ovary syndrome associating with different phenotypes. *Sci Rep*. 2017;7:14671.
- Hilker RE, Pan B, Zhan X, Li J. MicroRNA-21 enhances estradiol production by inhibiting WT1 expression in granulosa cells. *J Mol Endocrinol*. 2021;68:11–22.
- Bo Pan null. Julang Li null. MicroRNA-21 up-regulates metalloprotease by down-regulating TIMP3 during cumulus cell-oocyte complex in vitro maturation. *Mol Cell Endocrinol*. 2018;477:29–38.

41. Rezaq S, Huffman AM, Basnet J, Alsemeh AE, do Carmo JM, Yanes Cardozo LL, et al. MicroRNA-21 modulates brown adipose tissue adipogenesis and thermogenesis in a mouse model of polycystic ovary syndrome. *Biol Sex Differ*. 2024;15:53.
42. Pan B, Toms D, Shen W, Li J. MicroRNA-378 regulates oocyte maturation via the suppression of aromatase in Porcine cumulus cells. *Am J Physiol - Endocrinol Metabolism*. 2015;308:E525.
43. Khan HL, Bhatti S, Abbas S, Kaloglu C, Isa AM, Younas H, et al. Extracellular MicroRNAs: key players to explore the outcomes of in vitro fertilization. *Reprod Biol Endocrinol*. 2021;19:72.
44. Hu M, Lu Y, Zeng H, Zhang Z, Chen S, Qi Y, et al. MicroRNA-21 maintains hematopoietic stem cell homeostasis through sustaining the nuclear factor- $\kappa$ B signaling pathway in mice. *Haematologica*. 2020;106:412–23.
45. Wu T, Liu Y, Fan Z, Xu J, Jin L, Gao Z, et al. miR-21 modulates the immunoregulatory function of bone marrow mesenchymal stem cells through the PTEN/Akt/TGF- $\beta$ 1 pathway. *Stem Cells*. 2015;33:3281–90.
46. Ma J, Wu D, Yi J, Yi Y, Zhu X, Qiu H, et al. *Mir-378* promoted cell proliferation and inhibited apoptosis by enhanced stem cell properties in chronic myeloid leukemia K562 cells. *Biomed Pharmacother*. 2019;112:108623.

#### **Publisher's note**

Springer Nature remains neutral with regard to jurisdictional claims in published maps and institutional affiliations.